Distribution Agreement

In presenting this thesis or dissertation as a partial fulfillment of the requirements for an advanced degree from Emory University, I hereby grant to Emory University and its agents the non-exclusive license to archive, make accessible, and display my thesis or dissertation in whole or in part in all forms of media, now or hereafter known, including display on the world wide web. I understand that I may select some access restrictions as part of the online submission of this thesis or dissertation. I retain all ownership rights to the copyright of the thesis or dissertation. I also retain the right to use in future works (such as articles or books) all or part of this thesis or dissertation.

Signature:

_____ _____

Jingchan Yuan Date

Stochastic Modeling of TCDD Suppression of Terminal Differentiation of B Lymphocytes into Antibody-Secreting Cells

By

Jingchan Yuan
MSPH

Environmental Health

Qiang Zhang, PhD
Committee Chair

Stochastic Modeling of TCDD Suppression of Terminal Differentiation of B Lymphocytes into Antibody-Secreting Cells

By

Jingchan Yuan

Bachelor of Medicine
Sun Yat-sen University
2018

Thesis Committee Chair: Qiang Zhang, PhD

An abstract of
A thesis submitted to the Faculty of the
Rollins School of Public Health of Emory University
in partial fulfillment of the requirements for the degree of
Master of Science in Public Health
in Environmental Health
2020

Abstract

Stochastic Modeling of TCDD Suppression of Terminal Differentiation of B Lymphocytes into Antibody-Secreting Cells

By Jingchan Yuan

Background: Upon antigen encounter, naïve B lymphocytes are activated and differentiate to antibody-secreting plasma cells. Multiple transcriptional factors regulate this immune response, and 2,3,7,8-tetrachlorodibenzo-p-dioxin (TCDD) can suppress the process through interfering with the gene regulatory network. To better understand the systems-level mechanism and effect of TCDD on B lymphocyte terminal differentiation, we developed a stochastic mathematical model to simulate the molecular behavior underlying the process, based on previous literature and published studies. In the model when stimulated by the activator lipopolysaccharide (LPS), IRF4 is induced and coordinates with IRF8 to determine the cell fate. If LPS is strong enough, BCL6 would then be activated by IRF4 and initiate cell proliferation by inducing Myc and somatic hypermutation by inducing BACH2. However, when IRF4 reaches a higher level, BCL6 would instead be inhibited. Eventually, PRDM1 would be switched on with the drop of PAX5 through a coupled double-negative feedback loop. Through AhR-mediated repression of LPS-initiated signaling and augmentation of BACH2, TCDD can reduce the number of activated B cells and decrease the probability of differentiation. appropriately.

Result: Our result captured the expected dynamical changes in key transcription factors of B cells observed in mice stimulated by LPS. The B cell differentiation is an irreversible bistable switching process, and PRDM1 is the critical factor controlling the switch. It also illustrated a graded phenomenon with TCDD dose-response relationships. The numbers of IgM-positive cells and all living cells are generally more suppressed with increasing concentration of TCDD. The stochastic fluctuation in gene expression can modify the course of cellular trajectory and fate.

Conclusion: Most key events of terminal B lymphocytes differentiation were recapitulated by our model, but the quantitative prediction is limited due to the uncertainties within the model parameters. Therefore, further studies are required to explore the immune system as well as the disruption caused by TCDD and other dioxin-like compounds to make the model a useful tool for the risk assessment of dioxin's induced immunotoxicity.

Stochastic Modeling of TCDD Suppression of Terminal Differentiation of B Lymphocytes into Antibody-Secreting Cells

By

Jingchan Yuan

Bachelor of Medicine
Sun Yat-sen University
2018

Thesis Committee Chair: Qiang Zhang, PhD

A thesis submitted to the Faculty of the
Rollins School of Public Health of Emory University
in partial fulfillment of the requirements for the degree of
Master of Science in Public Health
in Environmental Health
2020

Table of Content

Introduction

2,3,7,8 – Tetrachlorodibenzo-p-dioxin (TCDD), one of the most biologically active members of the dioxin family, is commonly recognized as a persistent and ubiquitous environmental toxicant, which can be detected in air, water, and soil worldwide [1]. Through the activation of the aryl hydrocarbon receptor (AhR), TCDD and structurally-similar, dioxin-like compounds can target the immune system by suppressing the primary humoral immune response through impairing antigen-induced B cell differentiation into antibody-secreting plasma cells and consequently a decrease in immunoglobulin secretion [2].

Although the study regarding the health risk of TCDD has been conducted for years, the mechanism of the disruption caused by TCDD in the differentiation of B cells into antibody-producing plasma cells in the immune system is still not fully understood. A better systems-level understanding of the regulatory gene network underlying the B cell differentiation process will help to explain the effects of transcriptional and cellular events involved and their interference by environmental toxicants. Generally, when B cells receive stimulating signals from cell surface receptors including B-cell receptors (BCR), if the antigens are of high-affinity or abundant, B cells may be activated and differentiate into plasma cells directly However if the stimulation from the antigen is not strong enough or if the activation is T cell-dependent requiring co-stimulation by CD40 ligand and cytokines, signal transduction pathways such as the NF-κB pathway may be activated to promote B cell proliferation and selection of high-affinity antibodies in the Germinal Center (GC) [3]. The cell proliferation and differentiation in the GC response and how TCDD may disrupt it is the focus of our study.

In the T cell-dependent response, B cells can process and present the antigen through the surface molecule major histocompatibility antigen (MHC-II) to T follicular helper (Tfh) cells. The latter then produce multiple cytokines and CD40 ligand to induce the activation of B cells [4]. Then NF-κB, the critical transcription factor, is activated to induce transcription factor interferon

regulatory factor 4 (IRF4) and IRF8 [5]. The expression of IRF4 can also be induced by itself, forming a positive auto-regulatory feedback loop [6]. IRF4 and IRF8 are both members of the interferon regulatory factors that are identified in mammals and share similar structures [7]. Xu H etc. hypothesized that these two IRFs form a double-negative feedback loop by inhibiting each other's expression to determine the fate of B cell at the early stage, while meantime they play independent and distinctive role in other stages [7,8]. Induced IRF8 interacts directly with B cell lymphoma 6 (BCL6), thus enhancing BCL6 [9]. IRF4 has opposing effects for the regulation of BCL6. At the early GC B cell stage, an intermediate level of IRF4 can bind to BCL6 promoter to induce BCL6, while a higher level leads to the downregulation of BCL6 [8,10]. Increased IRF4 level above a critical threshold leads to the activation of PR domain containing 1 with zinc finger domain (PRDM1, also named as Blimp1) [11].

After IRF4 starts the initiation of B cell activation, sustained BCL6 is required to maintain the GC state [11]. BCL6 is the key regulator of GC reaction in which B cells can undergo somatic hypermutation (SHM) and class switch recombination (CSR) of their immunoglobulin (Ig) genes to increase the diversity and potential affinity of Ig [12]. Upregulated BCL6 in pre-GC B cells is required for the entry into the GC reaction, and then the development of cells toward terminal differentiation gradually represses the expression of BCL6 to terminate the cell growth and proliferation [13]. Therefore, the dynamic change in BCL6 links cellular proliferation and differentiation. Gitlin, etc. found that GC B cells tend to divide over six to eight times before exiting the cell cycle [14]. The size of B cell proliferative burst is controlled by the production of cell-cycle-regulating proto-oncoprotein Myc and the division stop as c-Myc drops to a certain level [15]. For the induction of Myc in the early phase, additional signals from Tfh cells and BCR are also transduced via NF-κB and FOXO1, respectively [16,17]. During the GC response, the clones of cells with higher affinity for the invading antigens are selected to expand and evade apoptosis, whereas other low-affinity clones are gradually lost [18].

PRDM1 is the master regulator to control the switch of GC B cells differentiating to plasmablasts. The core regulatory network contains two main coupled double-negative feedback loops comprising several transcriptional factors, including BCL6, PRDM1, and Paired Box 5 (PAX5) [19]. PRDM1 is a notable repressor for BCL6 and PAX5, and these two transcriptional factors are also able to inhibit PRDM1, which in turn silences Myc to terminate cell proliferation [20–24]. The mutual suppressions form a bistable switch that prevents the premature formation of plasma cells in the germinal center and avoid the reversion of plasma cells to B cells [20]. Of the regulatory network, PAX5 is highly expressed throughout the whole B cell stages and is only subsequently suppressed in terminal cell differentiation, hence it is recognized as the guardian of B cell identity and puts a brake on the secondary antibody-generating reaction [25,26]. Another function of PAX5 includes inhibition of IRF8 that suppresses BCR signals, therefore preventing early initiation of differentiation and neoplastic divisions by indirectly weakening the activation of PRDM1 [7,27].

Consistent with the requirement of cell divisions before differentiation, SHM is enhanced by the slowing of plasmablast generations, based on the observations that "the proportion of siblings identified with asymmetric fates is unchanged" [28]. BTB and CNC homology 2 (BACH2) was found to contribute to this "delay-driven diversity" mechanism [29]. It was demonstrated that BACH2-deficient GC B cells had lower drug-induced apoptosis and higher possibility of proliferation, which suggests that BACH2 acts as a transactivator for those checkpoint-regulator genes [30]. Activated by PAX5 and BCL6, BACH2 is able to repress PRDM1, and therefore reduces the probability of plasma cell differentiation and promotes the chance of forming high-affinity antibodies [31,32]. Furthermore, BCL6 and BACH2 are critical for SHM and CSR, as they are both positive regulators of activation-induced cytidine deaminase (AID) that is the initiator of SHM and CSR [33,34].

The immune toxic effects caused by TCDD and structurally similar compounds are mediated through the binding to AhR, a transcriptional sensor for xenobiotics [1]. By the suppression of activation protein 1 (AP-1), an important activator for PRDM1, via an AhR-dependent manner, TCDD-induced inhibition can result in dysregulation of PAX5, therefore, leading to significant inhibition of B cell activation and differentiation ultimately [35,36]. Besides the disconnection of signal transduction, TCDD is also able to enhance the expression of BACH2 which keeps repressing PRDM1 and continuous cell cycles; therefore, more B cells would be blocked from entering differentiation and eventual more cell death will ensue through apoptosis [28,37].

The process of gene expression is essentially stochastic, which may give rise to large fluctuations and rare events underpinning cell-to-cell variations [38,39]. Therefore, in this paper, we use a stochastic computational model to simulate the course of terminal B cell activation and differentiation and the effects of TCDD based on the structure and dynamical properties of the gene regulatory network as described above from the literature. We expect this model can at least partly represent the natural progress of humoral immune response and provide a biologically based framework for the dose-response assessment of dioxin immunotoxicity.

Method

Model Structure

Figure 1. Model Structure and Wiring Diagram

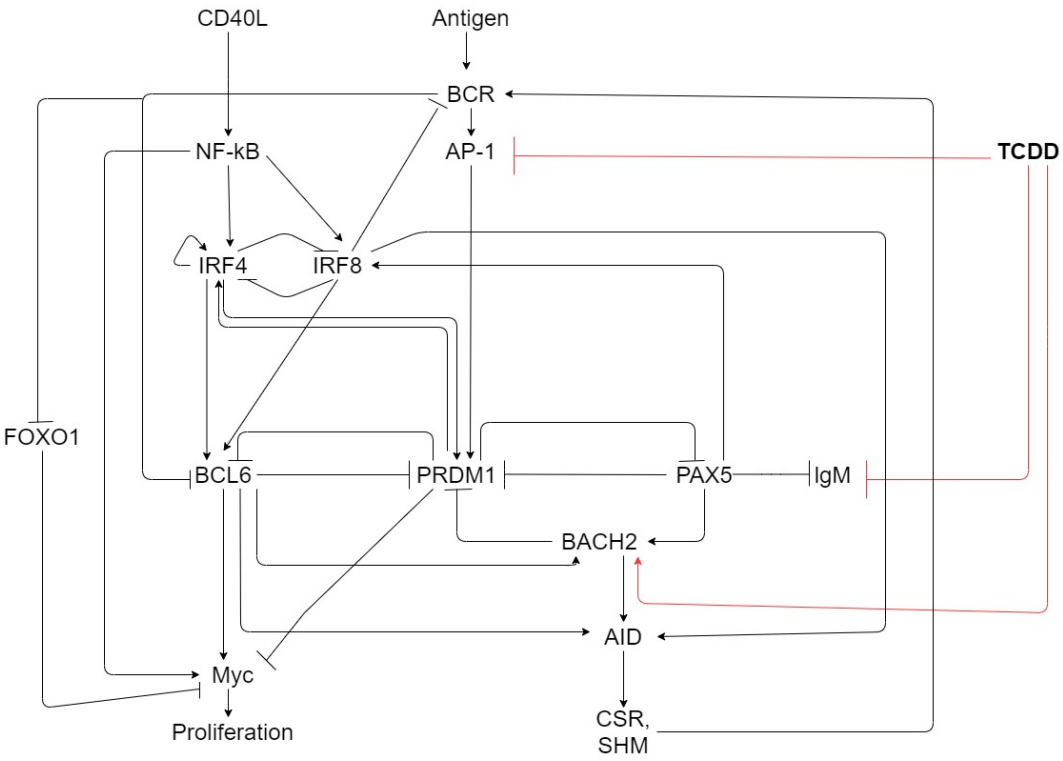

The model structure is illustrated in Figure 1. The gene expression simulated through the regulatory network involving IRF4, BCL6, PRDM1, PAX5, Myc, and BACH2 was based on the current understanding of stochastic gene expression and protein function studies [40]. To simplify the model, we limit the external stimulation to LPS, and include an intermediate signaling species S to collectively represent NF-κB and AP-1 here. So, LPS would activate IRF4 and IRF8 as well as, to some extent, PRDM1. The induction of IRF4 contains the auto-regulatory positive feedback loop and is suppressed by IRF8. Before IRF4 increases significantly, high expression of IRF8 keeps BCR from activated, therefore, reducing direct activation of PRDM1 through AP-1 and premature terminal differentiation. The double-negative feedback loop between IRF4 and IRF8,

as well as the downstream transcriptional factors, would coordinate to regulate the trajectories of B cells [7].

BCL6 determines the start of cell activation and proliferation of the GC response. BCL6 is at a relatively lower level before triggered by IRF4 and IRF8. The increase of BCL6 expression turns on Myc and AID expression for cell division and CSR/SHM. Other activation mechanisms from BCR, including repression of FOXO1 and activation of NF- κB, are not included in the model for simplicity. PRDM1 holds control of the competition between cell proliferation and differentiation. If it receives strong signals from BCR through AP-1, PRDM1 can be turned on directly, bypassing the regulation by IRFs and BCL6, which makes the immune response fast but with less efficient antibodies. If B cells are chronically exposed to TCDD, the AP-1 signal would not be that strong to directly differentiate B cells. The mutual enhancement between IRF4 and PRDM1 would accelerate the rising of PRDM1, which in turn, reverses the activation of BCL6. Moreover, the combined double-negative loop made up of BCL6, PRDM1, and PAX5 creates an irreversible bistable switch of gene expression. With the increase of PRDM1 and the downregulation of BCL6, the switch would be thrown to the "on" direction, where PRDM1 would experience a sharp rise and PAX5 and BACH2 decline correspondingly. A high level of PRDM1 then reinforce the suppression of Myc to suspend the cell cycle, and the remaining living cells would differentiate to plasma cells. Additionally, with BCL6 and BACH2 downregulated, CSR and SHM by AID are also terminated.

The immune toxicity of TCDD is through the binding to AhR, which then restrains AP-1 and upregulates BACH2. One study in mice also indicated that TCDD can contribute to the suppression of IgM by influencing the enhancer of immunoglobulin heavy chain [41]. But it is not included in the model because the effects may not be significant. The exact manner of the repression of AP-1 by TCDD-AhR complex remains unclear, and in this model, AP-1 is regarded

as a part of LPS-triggered signal S. Therefore, TCDD's effect on AP-1 is reflected as a reduction of S activated by LPS for simplicity.

Model implementation

Compared with deterministic models, stochastic models can add biological variations underlying the cell-to-cell differences observed in the cell differentiation process, making them suitable for gene network simulation. The network system is most likely to tend to the deterministic steady state at basal conditions, but near the threshold of activation, cellular behavior becomes divergent due to the stochastic gene expression noise. Some will switch to plasma cells and some remain as proliferating B cells. The computational model is coded and simulated in Julia 1.2.0 which allows us to easily switch between deterministic and stochastic solvers.

Ordinary differential equations, parameter values and initial conditions of the model are provided in Appendix Table S1-S3. Boolean logic describing the relationship between the states of cross-regulated transcription factors are shown in Appendix Table S4. Since this model structure involves multiple genes that regulate each other to reach stable steady states, their interactions cannot be recapitulated by simple additive terms. For example, before the initiation of B cell activation, IRF4 and PRDM1 remain low, while IRF8 and PAX5 have a high steady state, and BACH2 stays at an intermediately high level. After IRF4 is triggered and begins to rise to an intermediate level, BCL6 should be induced, but IRF8 is still highly expressed and PRDM1 remains repressed with increasing BACH2. When IRF4 reaches a higher threshold level, BCL6 should be suppressed as well as IRF8, while PRDM1 begins to increase with the drop of PAX5. These logical relationships are captured in Table S4.

The unit of variables in the model is copy numbers per cell. Cell size grows with the progression of the cell cycle. To maintain constant concentrations of mRNAs and proteins, we introduced a volume variable in the model to compensate for the differences in concentrations

due to cell growth and cell division [42]. This volume variable also serves as a mark for cell division when it reaches a randomly selected threshold. On average, the basal level of cell size is 100, and when the volume was induced to increase by Myc and reaches around 200, the cell would divide with each daughter cells inheriting nearly half of the volume and allocation of mRNAs and proteins to the two daughter cells following a binomial distribution.

To have an idea of the mRNA fluctuations in B cells, we examined the single-cell RNA sequencing data from mice stimulated by LPS for 3 days (unpublished data from Dr. Chris Scharer). As shown in Table 1 for IRF4, PRDM1 and BCL6 as examples, the absolute mRNA abundance in a single B cell is low, mostly a few copy numbers and, in many cases, is less than one molecule on average. For instance, during the process of differentiation, the mRNA of IRF4 changed from 0.25 to 7.51, while that of PRDM1 changed from 0.04 to 2.41, and BCL6 was also changing but at a much lower level. Therefore, due to the uncertainty of stochastic randomness, low abundance values are more likely to cause large fluctuations in protein levels, which can translate into noises meaningful for heterogeneous responses in the model. We used these single-cell data as our starting point for mRNA level parameterization but made upward adjustments if they are too low to achieve a stable steady state for B cells.

Table 1. Mean mRNA from single-cell RNAseq Study

Cluster	Number	IRF4		PRDM1		BCL6	
		Mean	S.td	Mean	S.td	Mean	S.td
1	651	0.25	0.57	0.04	0.22	0.06	0.24
2	888	0.25	0.54	0.11	0.62	0.03	0.20
3	1,505	0.55	1.48	0.18	0.63	0.08	0.40
4	375	1.94	3.37	0.49	1.15	0.38	0.88
5	2,884	7.51	7.22	2.41	2.65	0.004	0.06
6	509	4.15	4.28	2.56	3.04	0.01	0.13
7	790	0.44	0.95	0.16	0.62	0.03	0.21
8	764	0.81	2.07	0.30	1.00	0.14	0.54

Note: These single-cell RNA sequencing data were extracted from unpublished mouse B cells study from Dr. Chris Scharer lab. Cluster 1-2, 3-4, 5-6, 7-8 refer to resting B cells, activated B cells, plasma cells, and likely memory cells, respectively, at 72 h after LPS stimulation.

Result

Cell Response to LPS simulation

The behavior of the stochastic model, with the inherent randomness, does not entirely rely on the initial values of the variables. In this case, upon LPS stimulation, only a portion of cells could be activated and differentiate to plasma cells successfully, while others would continue to divide till the end of stimulation or stay quiescent.

Figure 2. Cell Volume Changes and Division after stimulation for LPS

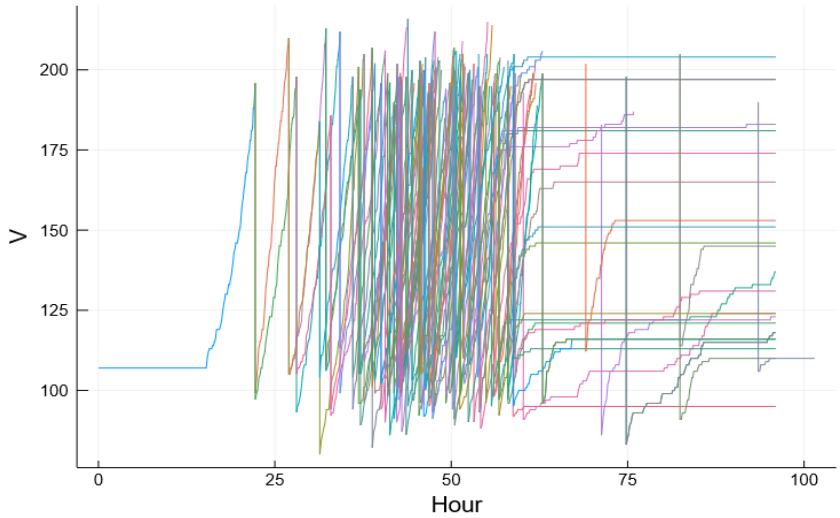

Figure 2. Volume changes of a B cell and its subsequent generations after stimulation by LPS=50. Only 20 cells were randomly selected from the 7th generation to 9th generation for visual clarity.

Figure 2 above showed the cell volume changes and cell division overtime after one B cell is stimulated by LPS. The first division took about 24 hours to occur, the second one spent about 3 hours, and subsequent ones are variable in doubling times. When cell division reaches the 8th or 9th generation after about 3 days, terminal differentiation occurs, and cells stop growing as reflected by the flat horizontal lines.

The output of the representative species protein is presented in Figure 3 (A-H). For the readability and clarity of the figures, we only choose one cell in the first generation as an example, and only 20 daughter cells were randomly selected from the 7th generation till the end of the simulation time. IRF4 protein had 2 levels during the process, as shown in Figure 3-A. The intermediate level in 30-60 hours reflects the activation by LPS, and then some cells moved to a higher level of IRF4 at about 60 hours heading to the plasma cells, while some cells remain at the intermediate level or in the process of heading to plasma cells without completing differentiation. By self-inducing, IRF4 determines the cell fate at the initial stage. As illustrated above, the intermediate level of IRF4 could induce BCL6, while the higher concentration inhibits it. Correspondingly, in our simulation, BCL6 rose to a relatively higher state at around 100 copy number compared with its basal steady level in B cells. This triggered Myc to initiate cell growth. Then, toward the end of 3-4 days, cells diverge into two fates: in some cells, BCL6 drops to nearly zero levels and ends up in the plasma cell state while others remain in the cell cycle with a high level of BCL6 (Figure 3-B). The decline of BCL6 also required the suppression of PRDM1 that acts as the master switch for cell differentiation.

In Figure 3-C, PRDM1 stayed at a low level until about 50 hours when the bistable switch was turned on. The fast climbing of PRDM1 not only accelerated the rise of IRF4, but contributed to the repression of BCL6 and Myc, and the fall of BACH2 through downregulation of PAX5, thus terminating cell proliferation and the naïve B cell state. As shown in Figure 3-D/E, PAX5 and BACH2 begin with a high level until some cells were switched on by PRDM1. PAX5 dropped down at 60 hours right after the separation of PRDM1 with different fate outcomes, and BACH2 decreased 2-3 hours later. IgM represented the ultimate output of the result of the whole regulatory network. According to Figure 3-F, as PAX5 diminished, IgM began to accumulate in cells, which have now become plasma cells.

The mRNA distribution of IRF4, PRDM1, and BCL6 by generation at 96 hours is illustrated in Figure 4, which was similar to the corresponding protein. The intermediate level of IRF4 mRNA was about 10 copy numbers per cell on average and was about 20 in the 8^{th} generation. mRNA of PRDM1 was barely expressed in earlier generations, then jumped to a level of about 10 on average. BCL6, as another essential regulatory factor, was highly expressed at 10 copy numbers per cell on average, then dropped to 0 in plasma cells. However, some cells failed to differentiate in which BCL mRNA and protein continued to be at high levels. The violin plots clearly demonstrated the high variability of mRNAs in individual cells.

The states of proteins in each cell at the end of 96 hours of stimulation by LPS are shown as violin plot in Figure 5. Because of stochastic gene expression, cells diverge in generations – some cells still remain in the early generations, some stay in the last generation but fail to switch to IgM-secreting plasma cells. In this circumstance, most cells manage to make to the $8^{th}/9^{th}$ generations, and about one third in these last two generations complete the terminal differentiation. IRF4 is the first species to start changing and by the $8^{th}/9^{th}$ generation, its upregulation is mostly obvious. IRF4 in the generations 5-7 are at the intermediate level. With respect to PRDM1, the separation of "on" and "off" state is relatively clear. Similar separation is also shown in the distribution of IgM, marking the formation of IgM-positive plasma cells in a fraction of cells in generations 8/9. Since the model does not make death as a fate, cells that fail to differentiate remain either in the early cell cycles or continue to survive in the $8^{th}/9^{th}$ generations.

In summary, the stochastic model captures the B cell proliferation and terminal differentiation observed in LPS-treated mice [43].

Figure 3. Simulated B Cell Response Activated by LPS

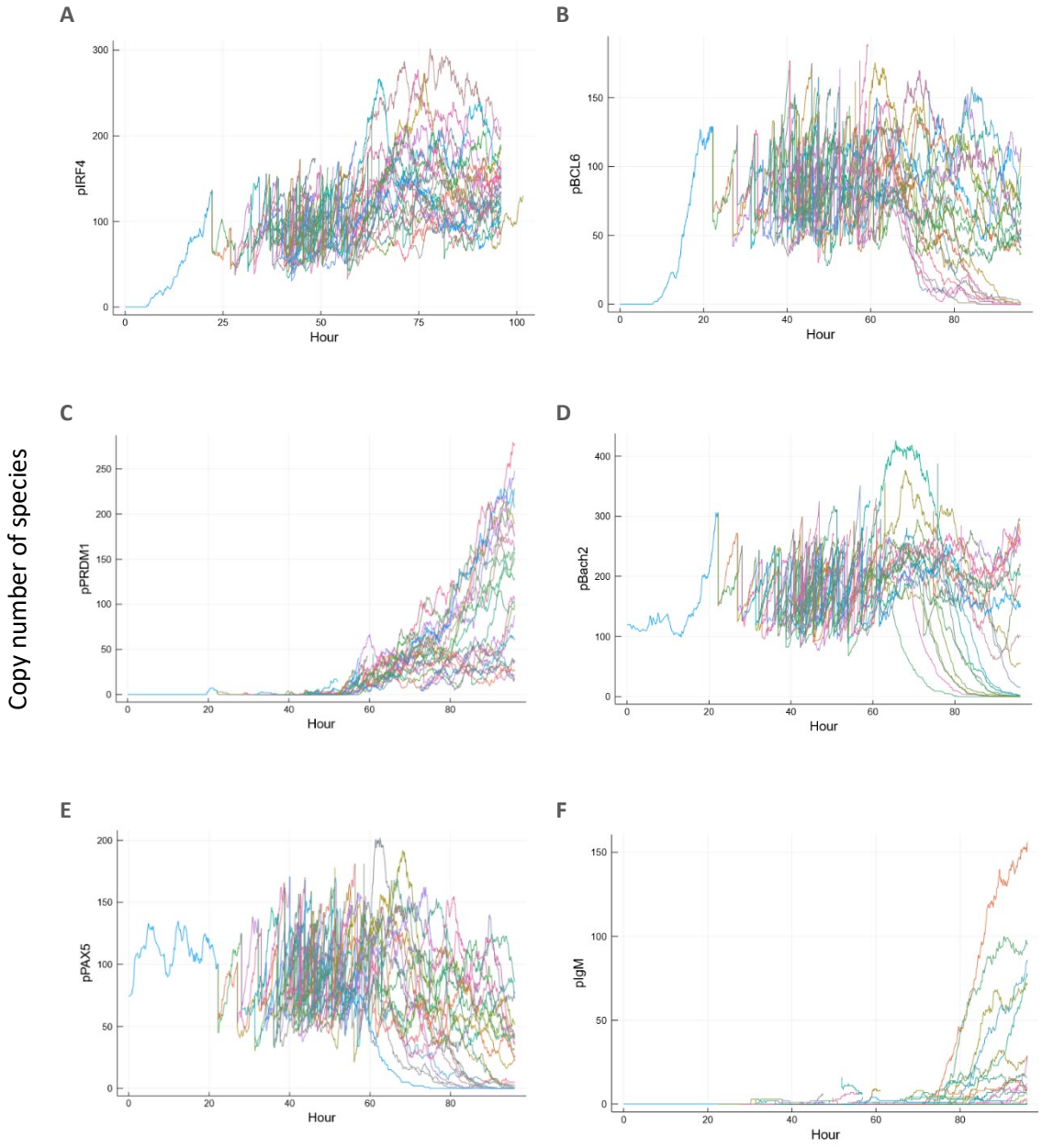

Figure 3. Simulated response of a B cell and its subsequent generations after stimulation by LPS=50. Data shown are dynamic changes in copy numbers of IRF4(A), BCL6(B), PRDM1(C), BACH2(D), PAX5(E), and IgM (F) proteins. For the readability and clarity of the figure, only 20 cells were randomly selected from the 7th generation to 9th generation.

Figure 4. Violin of mRNA of IRF4, PRDM1, and BCL6 by Generations

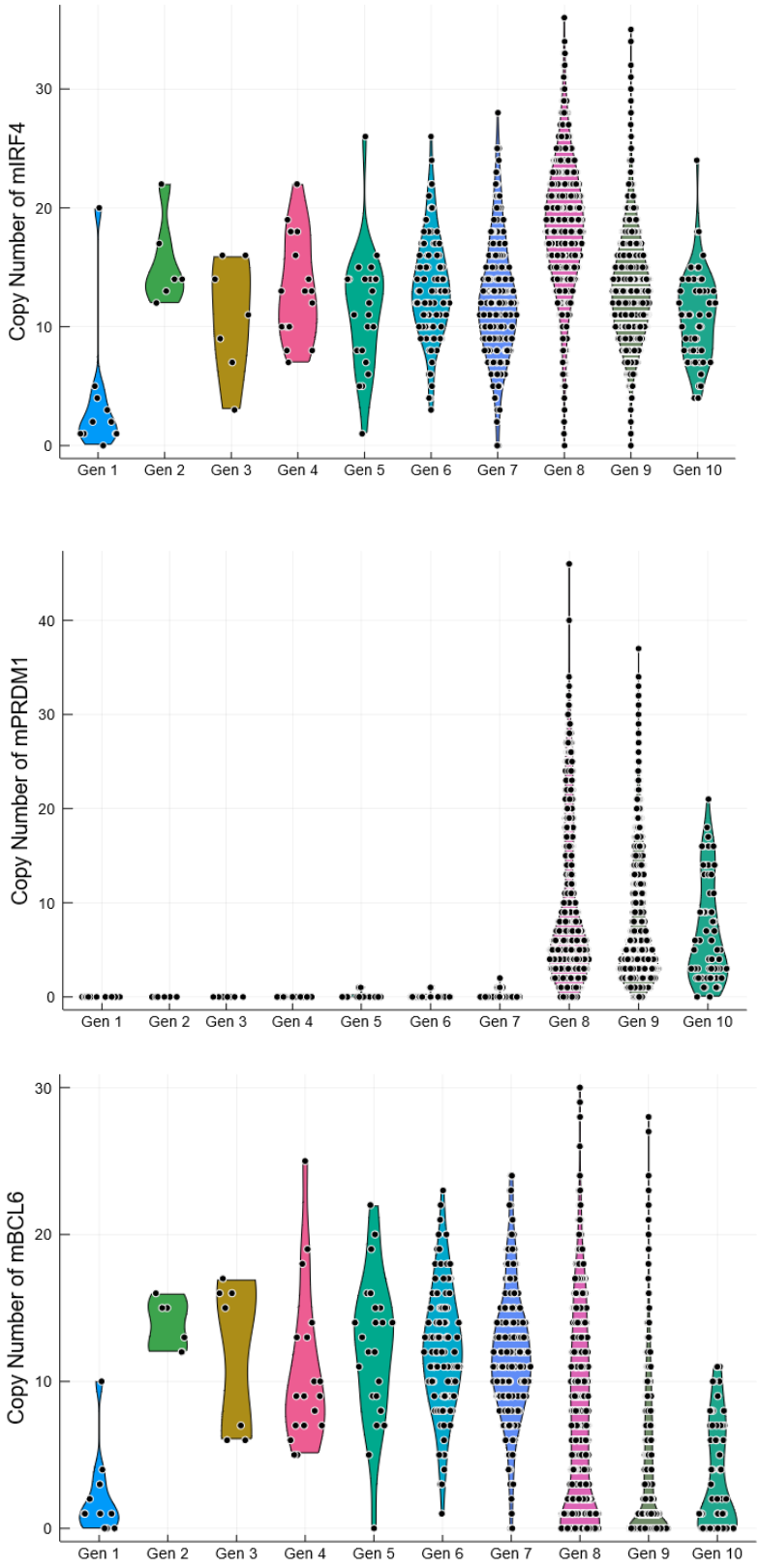

Figure 4. Violin Plot of mRNA of IR4, PRDM1 and BCL6 by Generations.

Data shown are mRNA levels in each cell in each generation for IRF4 (above), PRDM1 (middle), and BCL6 (below) after 100 initial B cells are stimulated by LPS=50 for 96 hours. Each point represents one single cell.

Figure 5. Violin Plot of Protein of IRF4, PRDM1 and IgM by Generations with LPS=50

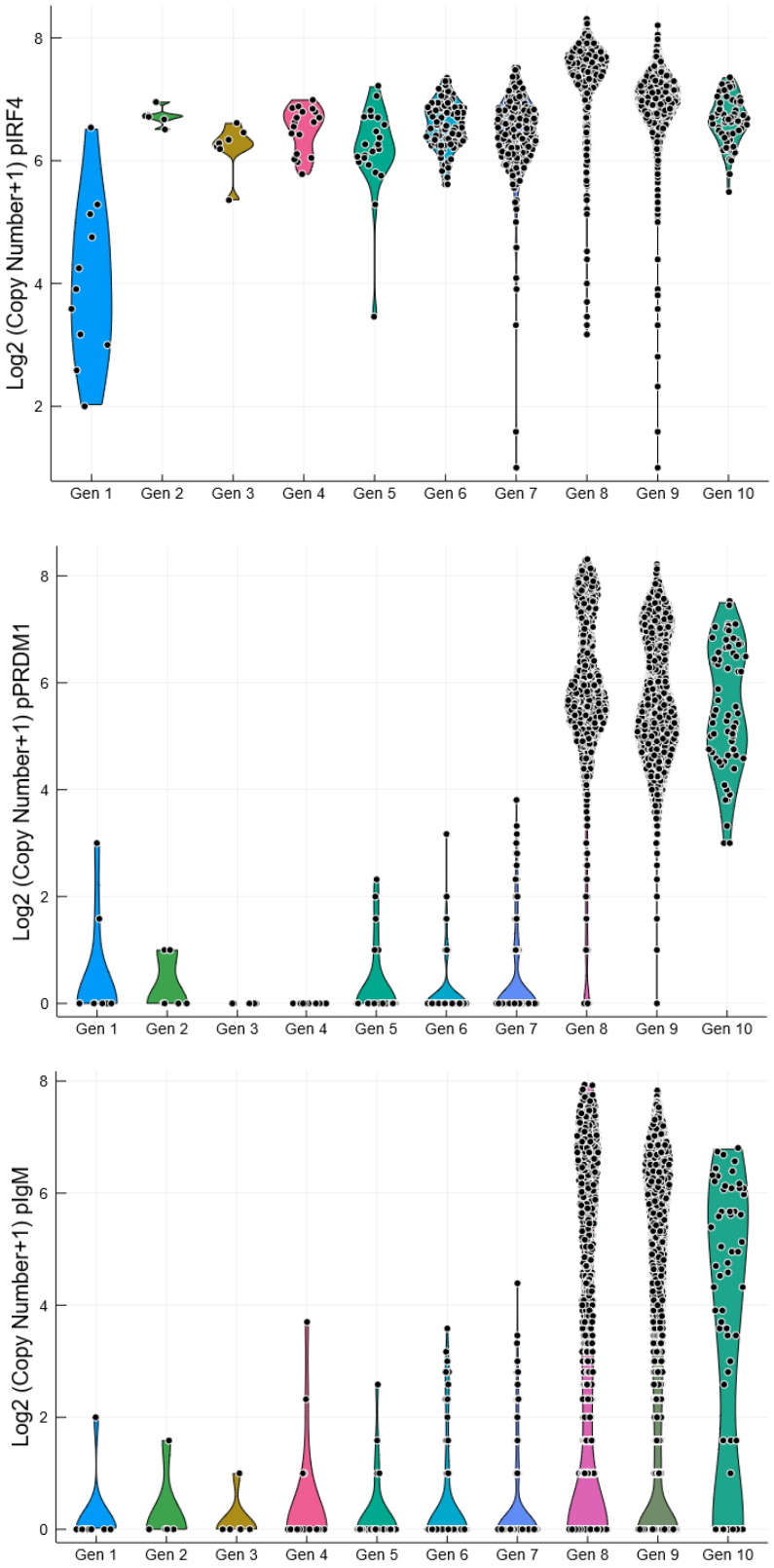

Figure 5. Violin Plot of Protein of IR4, PRDM1 and IgM by Generations with LPS=50.

Data shown are protein levels in each cell in each generation for IRF4 (above), PRDM1 (middle), and IgM (below) after 100 initial B cells are stimulated by LPS=50 for 96 hours. Each point represents one single cell.

Cell Response to LPS simulation in the presence of TCDD

We assessed the dose-response of TCDD with 8 different concentrations: 0.01, 0.1, 0.3, 1, 3, 10, 30 and 100 nM. Three concentrations were selected to illustrate the different degree of suppression by TCDD below.

Little suppression with TCDD = 0.1 nM

When the external conditions were LPS = 50 and TCDD = 0.1, the immune response was not influenced significantly, compared with no TCDD. The cell size and the timing of each species rise and fall seemed similar to the control at TCDD=0, despite the stochastic fluctuations. However, the emergence of IgM-positive cells had a slight delay, and the fluctuations of IRF4, PRDM1, and IgM seemed to have slight differences by the end of 96 hours (Figure 6). The majority of cells would enter and stay at generation 8/9, where the difference in IRF4 was more prominent. A relatively low IRF4-expressing subpopulation in generation 8 is present, which indicated that these cells had not initiated the differentiation process in the presence of TCDD. The distribution of PRDM1 and IgM had no apparent variance. It seemed that most cells in the generation 8/9 still accomplished the terminal switching or headed towards it. The production of IgM was not affected by this low concentration of TCDD.

Intermediate suppression with TCDD = 1 nM

When TCDD = 1 nM, the delay of cell proliferation and the suppression of cell differentiation became more significant, and the cell number and IgM-positive cells experienced a noticeable decrease at the end. The inhibition of LPS signaling by TCDD made the increase of IRF4 delayed until generation 4 to reach the intermediate level, while usually, this process would finish within the first generation (Figure 7). Nearly half of the cells in generation 8 cannot achieve a higher level of IRF4. As described above, a higher level of IRF4 would be required to inhibit BCL6, therefore, reducing the repression of PRDM1 and flipping the bistable switch to the “on” state.

Moreover, TCDD would undermine the effect of LPS on PRDM1 directly. Therefore, as shown in Figure 7, more cells tended to remain with a lower copy number of PRDM1 protein in generation 8/9 by the end of 96 hours, compared with the clear separation in the control. When PRDM1 was maintained at lower expression and the bistable switch could not be turned on, BCL6 and PAX5 remained at a higher state and sustained the induction of Myc and BACH2, which would result in continuous cell growth and divisions. More importantly, the disinhibition of PAX5 determines the secretion of antibodies, so, under the intermediate TCDD dose, the expression of IgM exhibits an evident decline. Cells in generation 8 barely transformed into plasma cells, while generation 9 seemed to proceed unaffectedly eventually. Therefore, if cells can advance to the 9^{th} generation in time unaffected by the delay caused by TCDD, they might complete the differentiation. However, other cells that were delayed in generations would have a low possibility of turning to plasma cells at the end.

High suppression with TCDD = 100 nM

When TCDD = 100 nM, the total number of cells at the end were much fewer (Figure 8). Most cells stayed in the 9th generation, and only about half of them would differentiate successfully.

Dose-response effect of TCDD

Within different TCDD doses, cells had various responses under stochastic gene expression conditions, which may not strictly correspond with the dose (Figure 9). To quantify the TCDD effect on IgM-positive cells, We set IgM > 20 as IgM-positive cells and counted their numbers, the number of total cells, and the percent of IgM-positive cells over total cells during the 96-h LPS-stimulated period in the presence of different concentrations of TCDD. As shown in figure 9, the number of IgM-positive cells and total living cells increased over time and they were pretty similar when TCDD = 0, 0.01, 0.1, and 0.3 nM. At TCDD = 1 nM, a slight decrease was observed with the number of IgM-positive cells compared with the lower TCDD dose groups. Then, at TCDD = 3 or 10 nM, there was an apparently lower number of IgM-positive cells and total cells,

compared with lower TCDD doses. At TCDD =30 and 100 nM, the lowest number of IgM positive cells and total cells were observed. The percentage of IgM-positive cells among all cells at each time point also increased over time and was suppressed by TCDD, suggesting that TCDD inhibited not only cell proliferation but also the terminal differentiation.

In summary, we found that the effect of TCDD on IgM-positive cell formation is dose-dependent and the effect becomes significant at 1 nM. Then, A higher dose could lead to more suppression in absolute numbers. When TCDD>30 nM, it exerted the most repression, and an even higher dose might not result in further changes. Such a dose response behavior reflected the nature of AhR-mediated response, which is saturated at high ligand concentrations.

Figure 6. Violin Plot of Protein of IRF4, PRDM1 and IgM by Generations with LPS=50 and TCDD = 0.1

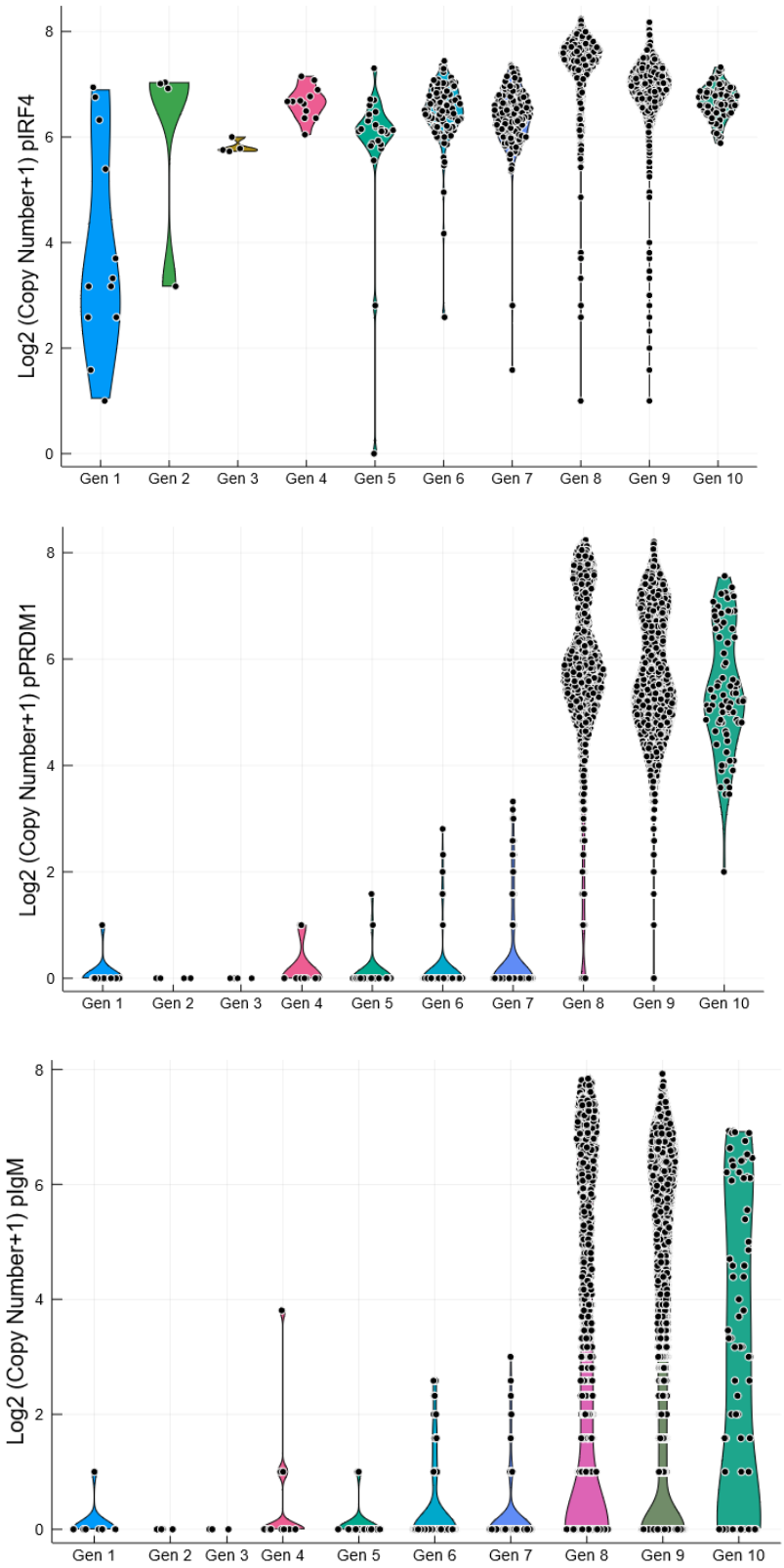

Figure 6. Violin Plot of Protein of IR4, PRDM1 and IgM by Generations with LPS=50 and TCDD=0.1.

Data shown are protein levels in each cell in each generation for IRF4 (above), PRDM1 (middle), and IgM (below) after 100 initial B cells are stimulated by LPS=50 and TCDD=0.1 for 96 hours. Each point represents one single cell.

Figure 7. Violin Plot of Protein of IRF4, PRDM1 and IgM by Generations with LPS=50 and TCDD = 1

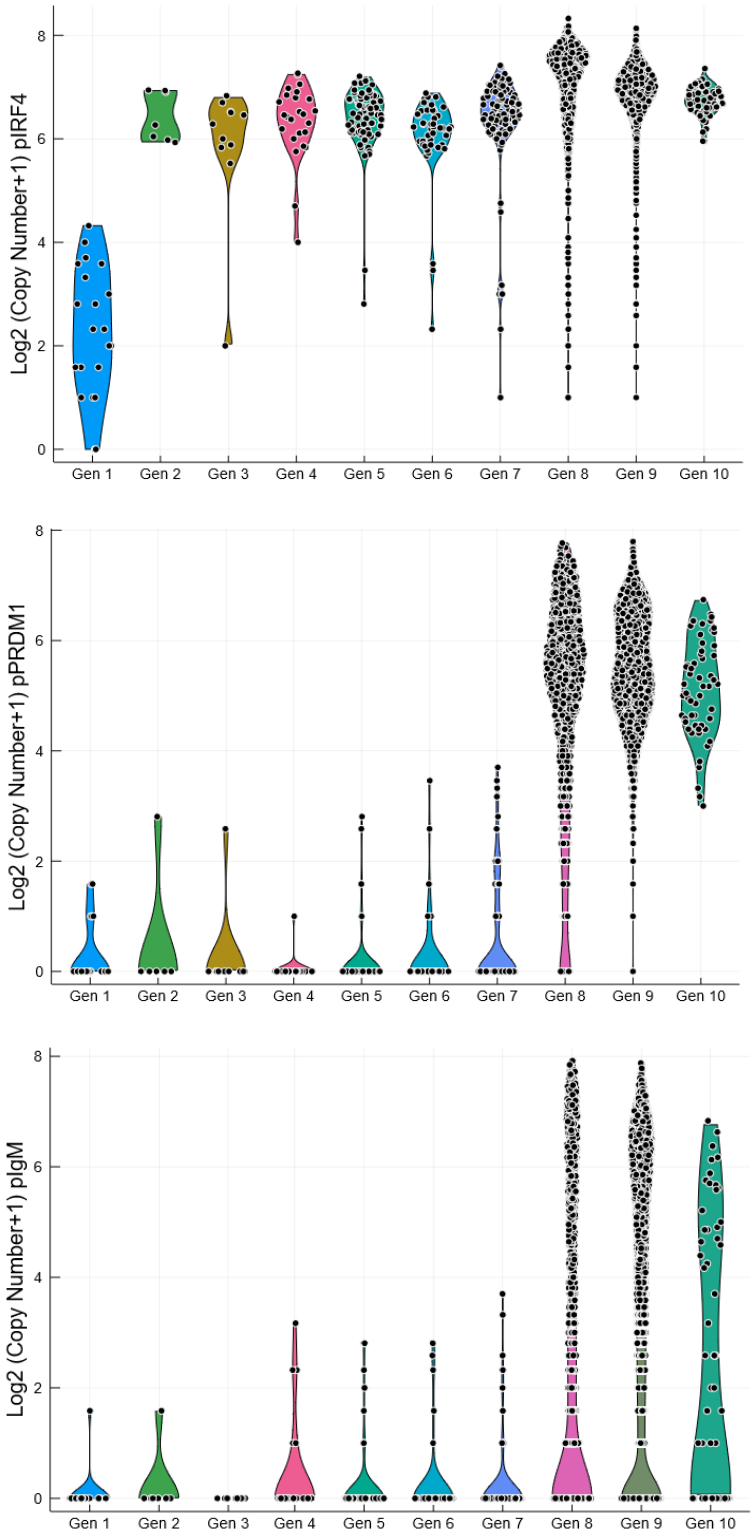

Figure 7. Violin Plot of Protein of IR4, PRDM1 and IgM by Generations with LPS=50 and TCDD=1.

Data shown are protein levels in each cell in each generation for IRF4 (above), PRDM1 (middle), and IgM (below) after 100 initial B cells are stimulated by LPS=50 and TCDD=1 for 96 hours. Each point represents one single cell.

Figure 8. Violin Plot of Protein of IRF4, PRDM1 and IgM by Generations with LPS=50 and TCDD = 100

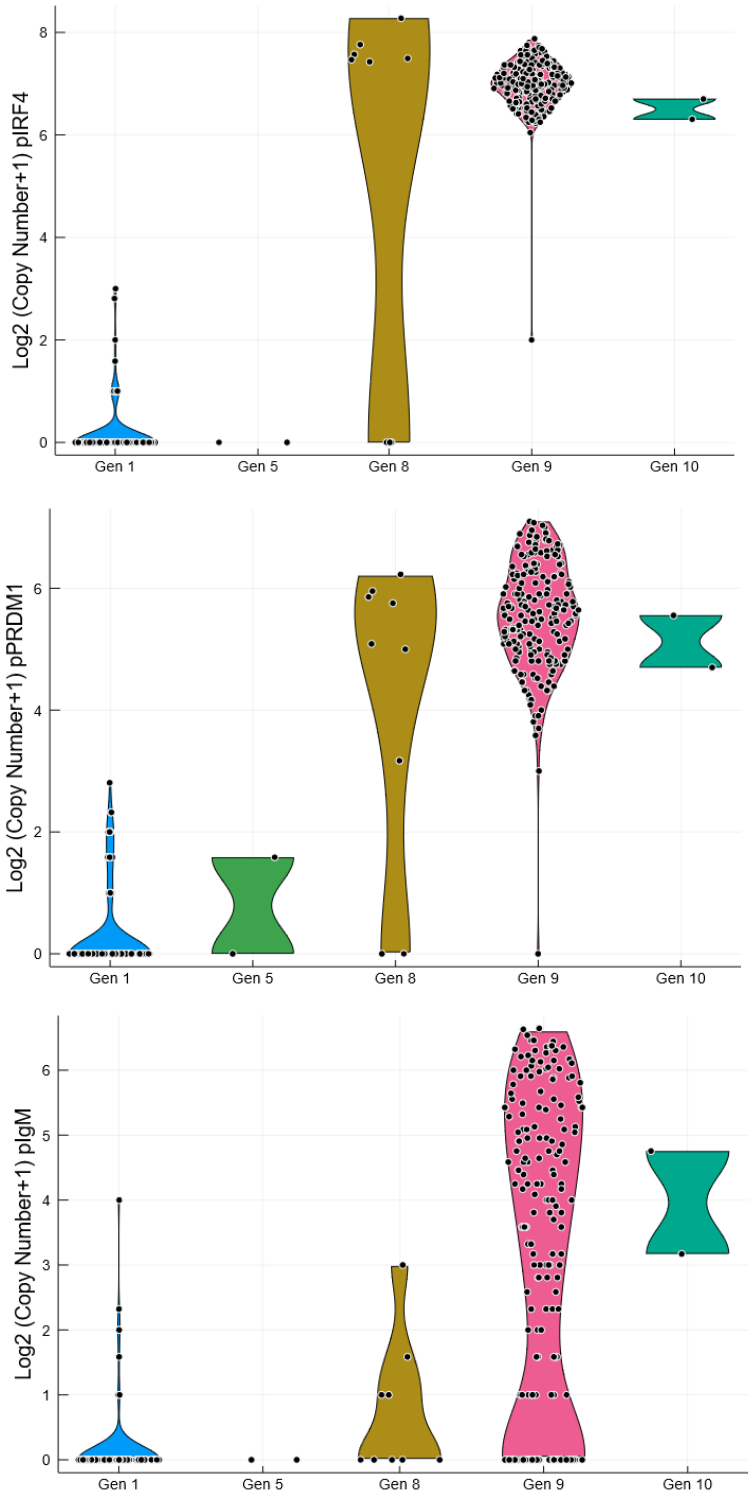

Figure 8. Violin Plot of Protein of IR4, PRDM1 and IgM by Generations with LPS=50 and TCDD=100.

Data shown are protein levels in each cell in each generation for IRF4 (above), PRDM1 (middle), and IgM (below) after 100 initial B cells are stimulated by LPS=50 and TCDD=100 for 96 hours. Each point represents one single cell.

Figure 9. Changes in the Number of IgM-positive Cells in the Presence of TCDD

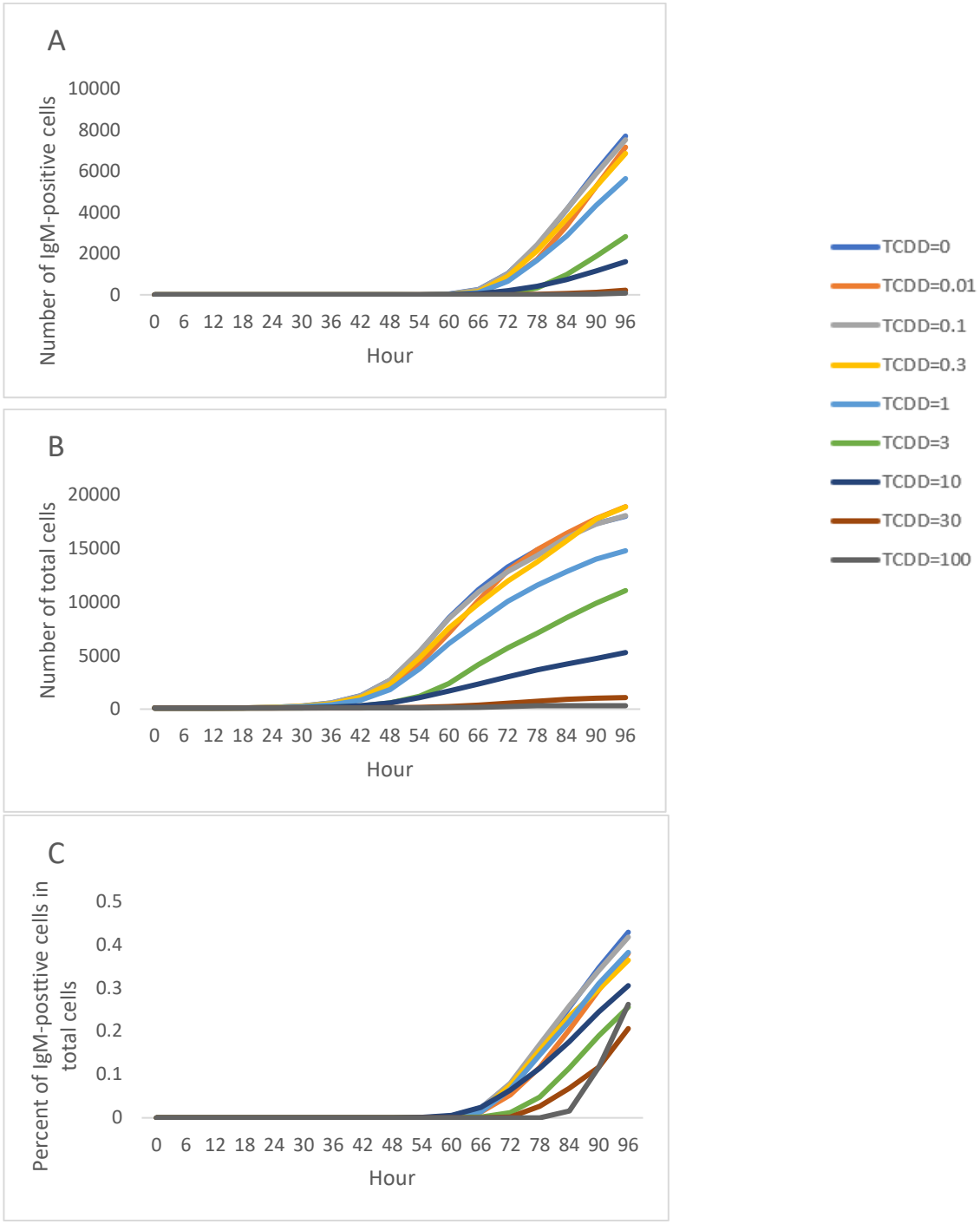

Figure 9. IgM-positive cells and total cells are inhibited by TCDD dose-dependently. The data were from simulations with LPS=50 and starting cell number = 100, in the presence of TCDD=0, 0.01, 0.1, 0.3, 1, 3, 10, 30, or 100 nM. IgM > 20 was considered as IgM-positive cells. The number of IgM-positive cells (A), total cells (B), and the percent of IgM-positive cells among total (C) at each time point were shown.

Discussion

The terminal differentiation from naive B cells to plasma cells is a bistable, irreversible process regulated by multiple transcription factors that interact with each other [19]. By developing stochastic models simulating the gene regulatory network in the B cell immune response, we can gain further insight into the sequence of events in this natural process at the molecular level and help to understand the effects of environmental immunotoxicant such as dioxin on Ig secretion. IRF4 is a primary activator for the B cell fate, which is almost silent in resting B cells, expressed at intermediate levels upon activation, and highly expressed in plasma cells [44]. Our stochastic model has recapitulated this expression profile of IRF4. Sustained high IRF4 level can antagonize the GC B cell status and promote the terminal differentiation of B cells [45]. During the rise of IRF4, BCL6 is induced to enhance Myc and to maintain the suppression of PRDM1. Therefore, BCL6 not only initiates cell proliferation but also prevents premature differentiation. In the meantime, BACH2 acts as a significant part of the delay mechanism for cell growth and antibody mutations. Our stochastic model has captured some of these features.

After a sufficient number of cell divisions, the binding motifs of the IRF4 shift, and BCL6 is instead inhibited.[45] The balance of the bistable switch moves towards to the "on" state when the repression of PRDM1 is weakening. The coupled double-negative feedback loop makes sure the irreversibility and stability of the bistable switch controlled by PRDM1. With the dropping of PAX5, the antibody is able to be produced and secreted. Additionally, as illustrated above, cell proliferation and differentiation are potential outcomes of "competing for timed stochastic fate," which hypothesized that cells need enough time to switch on the differentiation before the next division through faster cell transition within each generation, or slower division times. [46] Most cells would determine their fate by the 8th or 9th generation, according to our model simulation, which is in accordance with the behavior of mouse B cells stimulated by LPS.

Our results indicated a graded phenomenon in the TCDD dose-response relationship. Clearly, when TCDD<1 nM, there was no obvious repression, and when TCDD is between 1 to 30 nM, we could expect a graded decrease in cell activation and differentiation, respectively. However, when TCDD is pretty high, like > 30 nM, the effect of TCDD plateaued. The threshold of TCDD to inhibit the B cell response may be related to the bistable switches in the gene regulatory network. Moreover, TCDD caused the reduction of IgM by decreasing the relative number of IgM-positive cells, according to simulated results on the percent of IgM-positive cells among the total cells at each time point. This result is likely due to the induction of BACH by TCDD, at least in part, which makes the bistable switch harder to be flipped to the plasma cell state.

TCDD and other dioxin compounds disrupt B cell differentiation by the AhR pathway that is incompletely understood. Besides repressing BACH2, our model simulates TCDD as an inhibitor of the LPS-initiated signal, which will lead to a direct increase of LPS threshold for B cell activation. The dose-response curve also reveals the relationship between the increase of TCDD and the decrease of IgM-positive cells. However, in this circumstance, TCDD actually blunts cell activation by blocking the induction of IRF4 and PRDM1, which are normally activated by the LPS-stimulated signal. So, many simulated B cells would be stopped prior to proliferation. TCDD should otherwise act on the suppression of the differentiation stage.[36] For example, a cell should be able to enter and become stuck in the cell cycle with the inhibition by TCDD on differentiation. This limitation is probably because the model does not distinguish the signal from CD40L and BCR, so the TCDD now affects both activation and differentiation. Other possibilities include a more complex signal transduction network during the process of B cell presenting and receiving the antigen which was not explicitly modeled here. The TCDD dose-response provides a mechanistic explanation for the potential risk of TCDD accumulation in the human body since the suppressive effects may not be evident in the low-dose region if it is below a threshold.

The current work demonstrates a mechanistic modeling approach for understanding the gene regulatory network of B cells and how TCDD may disrupt this network to cause immunosuppression. The majority of key events of terminal B lymphocytes differentiating to antibody-secreting plasma cells were recapitulated by our model. However, the quantitative prediction is still limited, as many uncertainties exist with respect to model parameters. Some essential pieces of the pathways and transcription factors are not yet entirely understood with the lack of details. Further studies would be necessary to establish a more complete network model, which will allow us to better characterize the toxicodynamics of TCDD in humoral immune response.

Reference

1. Marshall NB, Kerkvliet NI. Dioxin and immune regulation: Emerging role of aryl hydrocarbon receptor in the generation of regulatory T cells. *Annals of the New York Academy of Sciences*. 2010;1183:25-37. doi:10.1111/j.1749-6632.2009.05125.x

2. Phadnis-Moghe AS, Crawford RB, Kaminski NE. Suppression of human B cell activation by 2,3,7,8-tetrachlorodibenzo-p-dioxin involves altered regulation of B cell lymphoma-6. *Toxicological Sciences*. 2015;144(1):39-50. doi:10.1093/toxsci/kfu257

3. Yu YH, Lin KI. Factors That Regulate the Generation of Antibody-Secreting Plasma Cells. In: *Advances in Immunology*. Vol 131. Academic Press Inc.; 2016:61-99. doi:10.1016/bs.ai.2016.03.001

4. Breitfeld D, Ohl L, Kremmer E, et al. *Follicular B Helper T Cells Express CXC Chemokine Receptor 5, Localize to B Cell Follicles, and Support Immunoglobulin Production*. Vol 192.; 2000. http://www.jem.org/cgi/content/full/192/11/1545.

5. Roy K, Mitchell S, Liu Y, et al. A Regulatory Circuit Controlling the Dynamics of NFκB cRel Transitions B Cells from Proliferation to Plasma Cell Differentiation. *Immunity*. 2019;50(3):616-628.e6. doi:10.1016/j.immuni.2019.02.004

6. Boddicker RL, Kip NS, Xing X, et al. The oncogenic transcription factor IRF4 is regulated by a novel CD30/NF-κB positive feedback loop in peripheral T-cell lymphoma. *Blood*. 2015;125(20):3118-3127. doi:10.1182/blood-2014-05-578575

7. Xu H, Chaudhri VK, Wu Z, et al. Regulation of bifurcating B cell trajectories by mutual antagonism between transcription factors IRF4 and IRF8. *Nature Immunology*. 2015;16(12):1274-1281. doi:10.1038/ni.3287

8. Shukla V, Lu R. IRF4 and IRF8: Governing the virtues of B lymphocytes. *Frontiers in Biology*. 2014;9(4):269-282. doi:10.1007/s11515-014-1318-y

9. Yoon J, Feng X, Kim YS, et al. Interferon regulatory factor 8 (IRF8) interacts with the B cell lymphoma 6 (BCL6) corepressor BCOR. *Journal of Biological Chemistry*. 2014;289(49):34250-34257. doi:10.1074/jbc.M114.571182

10. Basso K, Dalla-Favera R. BCL6. master regulator of the germinal center reaction and key oncogene in B Cell lymphomagenesis. In: *Advances in Immunology*. Vol 105. Academic Press Inc.; 2010:193-210. doi:10.1016/S0065-2776(10)05007-8

11. Ochiai K, Maienschein-Cline M, Simonetti G, et al. Transcriptional Regulation of Germinal Center B and Plasma Cell Fates by Dynamical Control of IRF4. *Immunity*. 2013;38(5):918-929. doi:10.1016/j.immuni.2013.04.009

12. Basso K, Dalla-Favera R. *Roles of BCL6 in Normal and Transformed Germinal Center B Cells*.

13. Kitano M, Moriyama S, Ando Y, et al. Bcl6 Protein Expression Shapes Pre-Germinal Center B Cell Dynamics and Follicular Helper T Cell Heterogeneity. *Immunity*. 2011;34(6):961-972. doi:10.1016/j.immuni.2011.03.025

14. Gitlin AD, Mayer CT, Oliveira TY, et al. HUMORAL IMMUNITY. T cell help controls the speed of the cell cycle in germinal center B cells. *Science (New York, NY)*. 2015;349(6248):643-646. doi:10.1126/science.aac4919

15. Heinzel S, Binh Giang T, Kan A, et al. A Myc-dependent division timer complements a cell-death timer to regulate T cell and B cell responses. *Nature Immunology*. 2017;18(1):96-103. doi:10.1038/ni.3598

16. Luo W, Weisel F, Shlomchik MJ. B Cell Receptor and CD40 Signaling Are Rewired for Synergistic Induction of the c-Myc Transcription Factor in Germinal Center B Cells. *Immunity*. 2018;48(2):313-326.e5. doi:10.1016/j.immuni.2018.01.008

17. Liu C, Banister CE, Weige CC, et al. PRDM1 silences stem cell-related genes and inhibits proliferation of human colon tumor organoids. *Proceedings of the National Academy of Sciences of the United States of America*. 2018;115(22):E5066-E5075. doi:10.1073/pnas.1802902115

18. Shlomchik MJ, Luo W, Weisel F. Linking signaling and selection in the germinal center. *Immunological Reviews*. 2019;288(1):49-63. doi:10.1111/imr.12744

19. Zhang Q, Bhattacharya S, Kline DE, et al. Stochastic modeling of B lymphocyte terminal differentiation and its suppression by dioxin. *BMC systems biology*. 2010;4:40. doi:10.1186/1752-0509-4-40

20. Shapiro-Shelef M, Calame KC. Regulation of plasma-cell development. *Nature Reviews Immunology*. 2005;5(3):230-242. doi:10.1038/nri1572

21. Crotty S, Johnston RJ, Schoenberger SP. Effectors and memories: Bcl-6 and Blimp-1 in T and B lymphocyte differentiation. *Nature Immunology*. 2010;11(2):114-120. doi:10.1038/ni.1837

22. Tellier J, Shi W, Minnich M, et al. Blimp-1 controls plasma cell function through the regulation of immunoglobulin secretion and the unfolded protein response. *Nature Immunology*. 2016;17(3):323-330. doi:10.1038/ni.3348

23. Mora-Ló Pez F, Reales E, Brieva JA, Campos-Caro A. Human BSAP and BLIMP1 conform an autoregulatory feedback loop. 2007. doi:10.1182/blood

24. Vasanwala FH, Kusam S, Toney LM, Dent AL. Repression of AP-1 Function: A Mechanism for the Regulation of Blimp-1 Expression and B Lymphocyte Differentiation by the B Cell Lymphoma-6 Protooncogene. *The Journal of Immunology*. 2002;169(4):1922-1929. doi:10.4049/jimmunol.169.4.1922

25. Fuxa M, Busslinger M. Reporter Gene Insertions Reveal a Strictly B Lymphoid-Specific Expression Pattern of Pax5 in Support of Its B Cell Identity Function . *The Journal of Immunology*. 2007;178(5):3031-3037. doi:10.4049/jimmunol.178.5.3031

26. Cobaleda C, Schebesta A, Delogu A, Busslinger M. Pax5: The guardian of B cell identity and function. *Nature Immunology*. 2007;8(5):463-470. doi:10.1038/ni1454

27. Pridans C, Holmes ML, Polli M, et al. Identification of Pax5 Target Genes in Early B Cell Differentiation. *The Journal of Immunology*. 2008;180(3):1719-1728. doi:10.4049/jimmunol.180.3.1719

28. Zhou JHS, Markham JF, Duffy KR, Hodgkin PD. Stochastically timed competition between division and differentiation fates regulates the transition from B lymphoblast to plasma cell. *Frontiers in Immunology*. 2018;9(SEP). doi:10.3389/fimmu.2018.02053

29. Igarashi Kyoko Ochiai Ari Itoh-Nakadai Akihiko Muto K, Kazuhiko Igarashi addresses, Ochiai K, Itoh-Nakadai A, Muto A, Igarashi Seiryo-machi K. *Orchestration of Plasma Cell Differentiation by Bach2 and Its Gene Regulatory Network*.; 2014. http://www.biotapestry.org/.

30. Swaminathan S, Huang C, Geng H, et al. BACH2 mediates negative selection and p53-dependent tumor suppression at the pre-B cell receptor checkpoint. *Nature Medicine*. 2013;19(8):1014-1022. doi:10.1038/nm.3247

31. Muto A, Tashiro S, Nakajima O, et al. The transcriptional programme of antibody class switching involves the repressor Bach2. *Nature*. 2004;429(6991):566-571. doi:10.1038/nature02596

32. Huang C, Geng H, Boss I, Wang L, Melnick A. Cooperative transcriptional repression by BCL6 and BACH2 in germinal center B-cell differentiation. *Blood*. 2014;123(7):1012-1020. doi:10.1182/blood-2013

33. Budzyńska PM, Kyläniemi MK, Kallonen T, et al. Bach2 regulates AID-mediated immunoglobulin gene conversion and somatic hypermutation in DT40 B cells. *European Journal of Immunology*. 2017;47(6):993-1001. doi:10.1002/eji.201646895

34. Basso K, Schneider C, Shen Q, et al. BCL6 positively regulates AID and germinal center gene expression via repression of miR-155. *Journal of Experimental Medicine*. 2012;209(13):2455-2465. doi:10.1084/jem.20121387

35. Suh J, Jeon YJ, Kim HM, Kang JS, Kaminski NE, Yang KH. Aryl hydrocarbon receptor-dependent inhibition of AP-1 activity by 2,3,7,8-tetrachlorodibenzo-p-dioxin in activated B cells. *Toxicology and Applied Pharmacology*. 2002;181(2):116-123. doi:10.1006/taap.2002.9403

36. Schneider D, Manzan MA, Yoo BS, Crawford RB, Kaminski N. Involvement of blimp-1 and AP-1 dysregulation in the 2,3,7,8-tetrachlorodibenzo-p-dioxin-mediated suppression of the IgM response by B cells. *Toxicological Sciences*. 2009;108(2):377-388. doi:10.1093/toxsci/kfp028

37. de Abrew KN, Phadnis AS, Crawford RB, Kaminski NE, Thomas RS. Regulation of Bach2 by the aryl hydrocarbon receptor as a mechanism for suppression of B-cell differentiation by 2,3,7,8-tetrachlorodibenzo-p-dioxin. *Toxicology and Applied Pharmacology*. 2011;252(2):150-158. doi:10.1016/j.taap.2011.01.020

38. Horowitz JM, Kulkarni R v. Stochastic gene expression conditioned on large deviations. *Physical biology*. 2017;14(3):03LT01-03LT01. doi:10.1088/1478-3975/aa6d89

39. Raj A, van Oudenaarden A. Nature, nurture, or chance: stochastic gene expression and its consequences. *Cell*. 2008;135(2):216-226. doi:10.1016/j.cell.2008.09.050

40. Zhang Q, Andersen ME, Conolly RB. Binary gene induction and protein expression in individual cells. *Theoretical biology & medical modelling*. 2006;3:18. doi:10.1186/1742-4682-3-18

41. Sulentic CEW, Zhang W, Na YJ, Kaminski NE. 2,3,7,8-Tetrachlorodibenzo-p-dioxin, an Exogenous Modulator of the 3'α Immunoglobulin Heavy Chain Enhancer in the CH12.LX Mouse Cell Line. *Journal of Pharmacology and Experimental Therapeutics*. 2004;309(1):71-78. doi:10.1124/jpet.103.059493

42. Padovan-Merhar O, Nair GP, Biaesch AG, et al. Single Mammalian Cells Compensate for Differences in Cellular Volume and DNA Copy Number through Independent Global Transcriptional Mechanisms. *Molecular Cell*. 2015;58(2):339-352. doi:10.1016/j.molcel.2015.03.005

43. Zhang Q, Kline DE, Bhattacharya S, et al. All-or-none suppression of B cell terminal differentiation by environmental contaminant 2,3,7,8-tetrachlorodibenzo-p-dioxin. *Toxicology and Applied Pharmacology*. 2013;268(1):17-26. doi:10.1016/j.taap.2013.01.015

44. Klein U, Casola S, Cattoretti G, et al. Transcription factor IRF4 controls plasma cell differentiation and class-switch recombination. *Nature Immunology*. 2006;7(7):773-782. doi:10.1038/ni1357

45. Ochiai K, Maienschein-Cline M, Simonetti G, et al. Transcriptional Regulation of Germinal Center B and Plasma Cell Fates by Dynamical Control of IRF4. *Immunity*. 2013;38(5):918-929. doi:10.1016/j.immuni.2013.04.009

Appendix

Table S1. Ordinary differential equations for model state variables

$$\frac{dV}{dt} = V \cdot \frac{k1 \cdot \left(pMyc \cdot \frac{100}{V}\right)^{n1}}{Kd1^{n1} + \left(pMyc \cdot \frac{100}{V}\right)^{n1}}$$

$$\frac{dS}{dt} = -k0 \cdot S$$

Initial Value of S: $\frac{dS}{dt} = LPS \cdot 20 \cdot \frac{Kd300}{TCDD_{dose} + Kd300}$

$$\frac{dmIRF4}{dt} = \frac{V}{V0} \cdot \left(k10 + \frac{k11 \cdot S}{Kd11 + S} + \frac{k12 \cdot \left(pIRF4 \cdot \frac{V0}{V}\right)^{n12}}{Kd12^{n12} + \left(pIRF4 \cdot \frac{V0}{V}\right)^{n12}} + \frac{k33 \cdot \left(pPRDM1 \cdot \frac{V0}{V}\right)^{n33}}{Kd33^{n33} + \left(pPRDM1 \cdot \frac{V0}{V}\right)^{n33}} \cdot \frac{k36 \cdot Kd36^{n36}}{Kd36^{n36} + \left(pIRF8 \cdot \frac{V0}{V}\right)^{n36}}\right)$$

$$\frac{dpIRF4}{dt} = k14 \cdot mIRF4 - k15 \cdot pIRF4$$

$$\frac{dmIRF8}{dt} = \frac{V}{V0} \cdot \left(k40 + \frac{k41 \cdot S}{Kd41 + S} + \frac{k42 \cdot Kd42^{n42}}{Kd42^{n42} + \left(pIRF4 \cdot \frac{V0}{V}\right)^{n42}} \cdot \frac{k43 \cdot \left(pPAX5 \cdot \frac{V0}{V}\right)^{n43}}{Kd43^{n43} + \left(pPAX5 \cdot \frac{V0}{V}\right)^{n43}}\right) - k44 \cdot mIRF8$$

$$\frac{dpIRF8}{dt} = k45 \cdot mIRF8 - k46 \cdot pIRF8$$

$$\frac{dmBCL6}{dt} = \frac{V}{V0} \cdot \left(k16 + k17 \cdot \frac{\left(pIRF4 \cdot \frac{V0}{V}\right)^{n13}}{Kd13^{n13} + \left(pIRF4 \cdot \frac{V0}{V}\right)^{n13}} \cdot \frac{Kd131^{n131}}{Kd131^{n131} + \left(pPRDM1 \cdot \frac{V0}{V}\right)^{n131}} \cdot \frac{Kd133^{n133}}{Kd133^{n133} + \left(pIRF4 \cdot \frac{V0}{V}\right)^{n133}} + \frac{k134 \cdot \left(pIRF8 \cdot \frac{V0}{V}\right)^{n134}}{Kd134^{n134} + \left(pIRF8 \cdot \frac{V0}{V}\right)^{n134}}\right) - k18 \cdot mBCL6$$

$$\frac{dpBCL6}{dt} = k19 \cdot mBCL6 - pBCL6 \cdot k20 \cdot \left(1 + \frac{v20 \cdot BCR}{Kd132 + BCR}\right)$$

$$\frac{dmPRDM1}{dt} = \frac{V}{V0} \cdot \left(k21 + k21 \cdot \frac{BCR}{Kd132 + BCR} + \frac{k35 \cdot S}{Kd35 + S} + \frac{k32 \cdot \left(pIRF4 \cdot \frac{V0}{V}\right)^{n32}}{Kd32^{n32} + \left(pIRF4 \cdot \frac{V0}{V}\right)^{n32}} \cdot \frac{k202 \cdot Kd202^{n202}}{Kd202^{n202} + \left(Division_{counter} \cdot \frac{V0}{V}\right)^{n202}} + \left(\frac{k34 \cdot Kd34^{n34}}{Kd34^{n34} + \left(pBach2 \cdot \frac{V0}{V}\right)^{n34}} + \frac{k22 \cdot Kd14^{n14}}{Kd14^{n14} + \left(pPAX5 \cdot \frac{V0}{V}\right)^{n14}}\right) \cdot \frac{k31 \cdot Kd31^{n31}}{Kd31^{n31} + \left(pBCL6 \cdot \frac{V0}{V}\right)^{n31}}\right) - k23 \cdot mPRDM1$$

$$\frac{dpPRDM1}{dt} = k24 \cdot mPRDM1 - k25 \cdot pPRDM1$$

$$\frac{dmBach2}{dt} = \frac{V}{V0} \cdot \left(k70 + \frac{k71 \cdot \left(pBCL6 \cdot \frac{V0}{V}\right)^{n71}}{Kd71^{n71} + \left(pBCL6 \cdot \frac{V0}{V}\right)^{n71}} + \frac{k72 \cdot \left(pPAX5 \cdot \frac{V0}{V}\right)^{n72}}{Kd72^{n72} + \left(pPAX5 \cdot \frac{V0}{V}\right)^{n72}} + \frac{k301 \cdot TCDD^{n301}}{Kd301^{n301} + TCDD^{n301}}\right) - k73 \cdot mBach2$$

$$\frac{dpBach2}{dt} = k74 \cdot mBach2 - k75 \cdot pBach2$$

$$\frac{dmPAX5}{dt} = \frac{V}{V0} \cdot \left(k26 + \frac{k27 \cdot Kd15^{n15}}{Kd15^{n15} + \left(pPRDM1 \cdot \frac{V0}{V}\right)^{n15}}\right) - k28 \cdot mPAX5$$

$$\frac{dpPAX5}{dt} = k29 \cdot mPAX5 - k30 \cdot pPAX5$$

$$\frac{dmMyc}{dt} = \frac{V}{V0} \cdot \left(k101 + \frac{k102 \cdot \left(pBCL6 \cdot \frac{V0}{V}\right)^{n102}}{Kd102^{n102} + \left(pBCL6 \cdot \frac{V0}{V}\right)^{n102}} \cdot \frac{k103 \cdot Kd103^{n103}}{Kd103^{n103} + \left(pPRDM1 \cdot \frac{V0}{V}\right)^{n103}} \cdot \frac{k202 \cdot \left(Division_{counter} \cdot \frac{V0}{V}\right)^{n202}}{Kd202^{n202} + \left(Division_{counter} \cdot \frac{V0}{V}\right)^{n202}}\right) - k104 \cdot mMyc$$

$$\frac{dpMyc}{dt} = k105 \cdot mMyc - k106 \cdot pMyc$$

$$\frac{dmAID}{dt} = \frac{V}{V0} \cdot \left(k80 + \left(\frac{k86 \cdot \left(pIRF8 \cdot \frac{V0}{V} \right)^{n86}}{Kd86^{n86} + \left(pIRF8 \cdot \frac{V0}{V} \right)^{n86}} + \frac{k81 \cdot \left(pBCL6 \cdot \frac{V0}{V} \right)^{n81}}{Kd81^{n81} + \left(pBCL6 \cdot \frac{V0}{V} \right)^{n81}} \right) \cdot \frac{k82 \cdot \left(pBach2 \cdot \frac{V0}{V} \right)^{n82}}{Kd82^{n82} + \left(pBach2 \cdot \frac{V0}{V} \right)^{n82}} \right) - k83 \cdot mAID$$

$$\frac{dpAID}{dt} = k84 \cdot mAID - k85 \cdot pAID$$

$$\frac{dmIgM}{dt} = \frac{V}{V0} \cdot \left(k90 + \frac{k91 \cdot Kd91^{n91}}{Kd91^{n91} + \left(pPAX5 \cdot \frac{V0}{V} \right)^{n91}} \right) - k92 \cdot mIgM$$

$$\frac{dpIgM}{dt} = k93 \cdot mIgM - k94 \cdot pIgM$$

Note: mVariable = mRNA of the species, pVariable = protein of the species

Table S2. Parameter values of the model

Parameter	Value	Note
V0	100	The original volume for cell size
k1	3.8508e−5	The growth rate of volume associated with
Kd1	25	Myc
n1	5	
k0	8.0225e−7	The degradation rate for S
k10	1.9254e−6	These parameters are associated with gene
k11	0.00019	expression of IRF4, in which k10 is the basal
Kd11	200	level, k11 and Kd11 controls the impacts of S,
k12	0.00019	k12, Kd12, n12 represents the IRF4 self-
Kd12	25	enhancing positive feedback loop, and k33,
n12	5	Kd33, n33, and k36, Kd36, n36 are associated
k33	0.00193	with the collective effect of PRDM1 and IRF8
Kd33	25	during the activation of IRF4.
n33	5	k14 is the translation rate from mRNA to
k36	1	protein, and k13, k15 is the degradation rate of
Kd36	25	mRNA, and protein, respectively.
n36	5	
k13	0.00019	
k14	0.00096	
k15	9.6270e−5	
k40	0.00039	These parameters are associated with gene
k41	0.00231	expression of IRF8, in which k40 is the basal
Kd41	200	level, k41 and Kd41 controls the impacts of S,
k42	1	and k42, Kd42, n42, and k43, Kd43, n43 are
Kd42	300	linked with the collective effect of the
n42	5	repression by IRF4 and induction by PAX5.
k43	0.00096	k45 is the translation rate from mRNA to
Kd43	25	protein, and k44, k46 is the degradation rate of
n43	5	mRNA and protein, respectively.
k44	0.00019	
k45	0.00096	
k46	9.6270e−5	
k16	1.9254e−6	These parameters are associated with gene
k17	0.00193	expression of BCL6, in which k16 is the basal
Kd13	25	level, k17, Kd13, n13, Kd133, n133, and
n13	5	Kd131, n131 regulate the collective effects of
Kd131	25	IRF4 and PRDM1 so that IRF4 can have
n131	5	concentration-dependent opposing effects on
Kd133	300	BCL6 where intermediate level promotes and
n133	5	high level suppresses BCL6. k134, Kd134,
k134	0.00019	n134 are associated with IRF8.
Kd134	200	k19 is the translation rate from mRNA to
n134	5	protein.
k18	0.00019	k18 is the degradation rate for mRNA
k19	0.00096	k20, v20, Kd132 is associated with the
v20	10	degradation rate of protein.
k20	9.6270e−5	
k21	7.7016e−6	These parameters are associated with the
Kd132	25	simulation of PRDM1, in which k21 is the
k35	7.7016e−7	basal level, k21, Kd132 reflects the influence
Kd35	200	of BCR, k35, Kd35 are associated with S, k32,
k32	0.00058	Kd32, n32, and k202, Kd202, n202 are to let
Kd32	25	IRF4 regulate the activation of PRDM1 that

n32	5	would not happen in the first 8 cell divisions.
k202	1	K34, Kd34, n34, k22, Kd14, n14, and k31,
Kd202	120	Kd31, n31 represent the collective effects of
n202	6	the suppression by BACH2, PAX5, and
k34	0.5	BCL6, respectively, which would create the
Kd34	25	coupled double-negative feedback loop as
n34	5	described.
k22	0.5	k24 is translation rate.
Kd14	25	k23, and k25 are the degradation rate for
n14	5	mRNA and protein, respectively.
k31	0.00193	
Kd31	25	
n31	5	
k23	0.00019	
k24	0.00096	
k25	9.6270e−5	
k26	9.6270e−6	These parameters are associated with the
k27	0.00193	expression of PAX5, in which k26 is the basal
Kd15	25	level, and k27, Kd15, n15 are associated with
n15	5	the repression by PRDM1
k28	0.00019	k29 is the translation rate.
k29	0.00096	k28, and k30 are the degradation rate for
k30	9.6270e−5	mRNA, and protein, respectively.
k101	1.9254e−6	These parameters are associated with the gene
k102	0.00193	expression of Myc, in which k101 is the basal
Kd102	25	level, k102, Kd102, n102, and k103, Kd103,
n102	5	n103 are associated with the collective effects
k103	1	by BCL6 and PRDM1. k202, Kd202, n202 are
Kd103	25	also involved to make sure the cell growth
n103	5	would not start until the 8th cell division.
k104	0.00019	k105 is the translation rate.
k105	0.00096	k104, and k106 are the degradation rate for
k106	9.6270e−5	mRNA and protein, respectively.
k70	1.9254e−6	These parameters are associated with the gene
k71	0.00193	expression of BACH2, in which k70 is the
Kd71	25	basal level, k71, Kd71, n71 reflect the
n71	5	induction by BCL6, k72, Kd72, n72 are linked
k72	0.00193	with tPAX5, and k301, Kd301, n301 mediate
Kd72	25	the impact caused by TCDD.
n72	5	k74 is the translation rate.
k301	0.00193	k73, and k75 are degradation rate for mRNA,
Kd301	1	and protein, respectively.
n301	1	
k73	0.00019	
k74	0.00096	
k75	9.6270e−5	
k80	7.7016e−7	These parameters are associated with the gene
k86	0.00077	expression of AID, in which k80 is the basal
Kd86	200	level, k86, Kd86, n86, and k81, Kd81, n81 can
n86	5	represent the collective effects by IRF8, and
k81	0.00077	BCL6, respectively, and k82, Kd82, n82 are
Kd81	25	associated with BACH2. So, it can exhibit the
n81	5	dual activation from IRF8 and BCL6, while
k82	1	BACH2 have the most contribution to the rise
Kd82	25	of AID.
n82	5	k84 is the translation rate.

k83 k84 k85	7.7016e−5 0.00193 0.00019	k83, and k85 are the degradation rate for mRNA AID and protein AID, respectively.
k90 k91 Kd91 n91 k92 k93 k94	3.8508e−7 0.00039 25 6 3.8508e−5 0.00039 3.8508e−5	These parameters are associated with the gene expression of IgM, in which k90 is the basal level, and k91, Kd91, n91 can control the suppression by PAX5. k93 is the translation rate k92, and k94 are the degradation rate for mRNA and protein, respectively.
k200 k201	0.00019 1.9254e−8	These parameters are associated with a factor that is designed to make sure that differentiation would not be triggered before 8^{th} cell cycles.
k300 Kd300	1 1	These parameters are used to estimate the effect of TCDD on LPS-initiated signal S at the start of stimulation.
TCDD	0	The value may vary.
BCR	0	For simplicity, BCR is limited to 0.
LPS	50	The initial stimulatory signal for the model.

Note: Most values of parameters are unknown. Therefore, they are either estimated from relevant mouse studies or general knowledge in the literature.

Table S3. Average initial steady-state levels of all molecular species in the model

Molecular Species	Initial Steady-State Value	
	Mean	Standard Deviation
IRF4 mRNA	0	0
IRF4 protein	0.03	0.17
IRF8 mRNA	7.09	2.61
IRF8 protein	70.35	16.95
BCL6 mRNA	0.02	0.14
BCL6 protein	0.16	0.63
PRDM1 mRNA	0.03	0.17
PRDM1 protein	0.51	1.36
Myc mRNA	0.02	0.14
Myc protein	0.29	1.33
BACH2 mRNA	10.28	3.21
BACH2 protein	99.34	10.73
PAX5 mRNA	10.15	2.79
PAX5 protein	102.65	20.76
AID mRNA	0.07	0.29
AID protein	0.72	2.30
IgM mRNA	0.02	0.14
IgM protein	0.15	0.67
Volume	99.83	3.50
S	0	0
TCDD	0	0

Note: Each value represents the average copy number of molecules per cell. The stochastic model was first allowed to run for 24 hours to reach steady state; then these values were obtained by taking the mean of 100 cells with their standard deviation, when the stimulation signal S, and TCDD were set to 0.

Table S4. Boolean logic relationship among genes in the model

		Species	Naïve B cells	Differentiation	Plasma cells
Input	Activator	S	1	0	0
	Activator	IRF4	0	1	2
	Activator	PRDM1	0	0	1
	Repressor	IRF8	1	2	1
Output		IRF4	0	1	2
Note	**IRF4 = S + IRF4 + PRDM1 × IRF8**				
Input	Activator	S	1	0	0
	Activator	PAX5	1	1	0
	Repressor	IRF4	0	1	2
Output		IRF8	1	2	1
Note	**IRF8 = S + IRF4 × PAX5**				
Input	Activator	IRF4	0	1	2
	Activator	IRF8	1	2	1
	Repressor	PRDM1	0	0	1
	Repressor	IRF4	0	1	2
Output		BCL6	0	1	0
Note	**BCL6 = IRF4 (activator) × PRDM1 × IRF4 (repressor) + IRF8**				
Input	Activator	S	1	0	0
	Activator	IRF4	0	1	1
	Repressor	BACH2	1	2	1
	Repressor	PAX5	1	1	0
	Repressor	BCL6	0	1	0
Output		PRDM1	0	0	1
Note	**PRDM1 = S + IRF4 + (BACH2 + PAX5) × BCL6**				
Input	Activator	BCL6	0	1	0
	Repressor	PRDM1	0	0	1
Output		Myc	0	1	0
Note	**Myc = BCL6 × PRDM1**				
Input	Activator	BCL6	0	1	0
	Activator	PAX5	1	1	0
	Activator	TCDD	-	-	-
Output		BACH2	1	2	1
Note	**BACH2 = BCL6 + PAX5 + TCDD**				
Input	Activator	IRF8	1	2	1
	Activator	BCL6	0	1	0
	Activator	BACH2	1	2	1
Output		AID	0	1	0
Note	**AID = (IRF8 + BCL6) × BACH2**				

Note: 1, 2 represents the intermediate and higher level of gene expression, respectively, and 0 represents no or low expressions. The output of PAX5 and IgM simply depends on PRDM1 and PAX5, respectively. So, they are not included in the table. In the naïve B cells before the activation, only IRF8, BACH2 and PAX5 are highly expressed. During the activation and differentiation process, IRF4, BCL6, Myc, and AID increase from 0 to level 1, while IRF8 and BACH2 reach level 2. Eventually, IgM emerges from level 0 to 1, IRF4 increased to level 2, IRF8, Myc, BCL6, BACH2 and AID drops to level 0, and PRDM1 rises to level 1 with the drop of PAX5 to level 0 in the plasma cells. These logics here indicate the mathematical relationship among species in the computational model, with the details of equations shown in Table S1.